Egypt. J. Chem. **Vol. 66**, No. SI 13. pp. 2279 - 2290 (2023)

Egyptian Journal of Chemistry

http://ejchem.journals.ekb.eg/

Enforcement of Ceftriaxone – PAM-18Na Polymer Nanoformula Versus Streptococcus pneumonia and Klebsiella pneumonia –as Pulmonary Pathogenic Bacteria

Asmaa Atef[a], Mohamed I. Zanaty[a], Zienab E. Eldin[b], Basma H. Amin[c], Ahmed A. Hamed[d], Ahmed O. El-Gendy[e]*, Ahmed A. G. El-Shahawy[b]

[a]*Department of Biotechnology, Faculty of Postgraduate Studies for Advanced Sciences (PSAS), Beni-Suef University, Beni-Suef 62511, Egypt.*

[b]Materials Science and Nanotechnology Department, *Faculty of Postgraduate Studies for Advanced Sciences (PSAS), Beni-Suef University, Beni-Suef 62511, Egypt.*

[c]*The Regional Center for Mycology and Biotechnology (RCMB), Al-Azhar University, Nasr City, Cairo11787, Egypt.*

[d] *Microbial Chemistry Department, National Research Centre, 33 El-Buhouth Street, Dokki, Giza 12622, Egypt.*

[e] *Microbiology and Immunology Department, Faculty of Pharmacy, Beni-Suef University, Beni-Suef 62511, Egypt.*

Abstract

Ceftriaxone is one of the most often prescribed antibiotics for treating the majority of fatal bacterial infections. By forming a nanostructured complex between PAM-18Na polymer and common drugs, one can reduce drug consumption and lessen the adverse effects of the medicine. This study looked at the efficacy of a nanostructured formula containing Ceftriaxone-PAM-18Na for eradicating Streptococcus pneumonia and Klebsiella pneumonia. The dispersion method was applied to prepare the formula. The characterization of the polymer, ceftriaxone, as well as the formula, was done by XRD, FTIR, Zeta-sizer, and Zeta potential. Thermal characterization and morphology detection using a high-resolution transmission electron microscope were done for the formula. Compared to drug or polymer, antibacterial testing of the formula revealed the highest inhibition zones against Gram-positive and Gram-negative pulmonary bacterial infections (18.0 ± 0.32 and 13.0 ± 0.51 mm, respectively). Ultrastructural examination revealed the dramatic effect of the synthesized formula on the structure of Streptococcus pneumonia and Klebsiella pneumonia. The synthesized formula had a cytotoxic concentration of CC50 = 960.12 ± 29.04 µg/mL when tested on MRC-5 mammalian cells (normal human lung fibroblast cells), indicating its safety at clinically used concentrations. Our findings suggest that the PAM-18Na polymer can potentially improve Ceftriaxone's ability to eradicate pathogenic lung bacteria as a follow-up treatment option for resistant strains.

Keywords: Antimicrobial activity, nano-complex, Streptococcus pneumonia, Klebsiella pneumonia, Ceftriaxone, PAM-18Na polymer.

1. Introduction

In light of the high rates of morbidity and mortality attributed to pathogenic bacterial infections, as well as the rising costs associated with patient healthcare, this issue has major public health implications [1]. Antimicrobial therapy alternatives are numerous; however, due to the prevalence of germs that are resistant to medications, their effectiveness is limited. Numerous traditional antibiotics have been unable to significantly enhance the overall life expectancy of individuals with

*Corresponding author e-mail: ahmed.elgendy@pharm.bsu.edu.eg. (Ahmed O. El-Gendy)
Received date 15 January 2023; revised date 15 May 2023; accepted date 05 June 2023
DOI: 10.21608/EJCHEM.2023.187613.7457

infectious diseases [2]. The main causes of antibiotic resistance (AMR), which frequently lowers the effectiveness of recently discovered antibiotics and their derivatives, are abuse and overuse of these medications [3]. The AMR develops naturally, but the abuse of antibiotics in both people and animals has sped up the process [4]. About 700,000 people die each year from antibiotic-resistant diseases, and it's predicted that number could rise to nearly 10 million by the year 2050, creating a global health disaster of AMR. [3, 5]. According to the WHO, AMR has been linked to an increase in hospitalization, higher medical expenses, and elevated death rates. The successful management of infections brought on by drug-resistant microorganisms is threatened by AMR [5].

Research efforts in a variety of domains, notably biochemistry, nanotechnology, pharmacology, and cell biology, have led to the development of nanocarrier drug delivery technologies [6, 7]. The nanoparticles can either act as antibacterial agents or as transporters for antibiotic drugs, increasing both the bioavailability and efficacy of the antibiotics [8]. Antibacterial nanoparticles are made from a variety of components, such as metals and chitosan, and can destroy bacterial membranes [9]. Another tactic to improve the absorption and elimination of bacteria is the encapsulation of antibiotic medications into nanocarriers. Nanocarrier systems increase the effectiveness of antibiotics and decrease their hazards compared to traditional therapy [10, 11].

It has previously been observed that the sodium salt of poly (maleic acid-alt-octadecene), known here as PAM-18Na, can help boost the potency of antimicrobial compounds against resilient bacterial species [12, 13]. A third-generation cephalosporin antibiotic called ceftriaxone is used to treat a variety of pathogenic bacteria, most notably lower respiratory tract infections that are mostly brought on by certain pulmonary pathogenic bacteria [14, 15]. This study aimed to investigate the antibacterial impact of a synthesized and characterized nanoformula of ceftriaxone antibiotic-loaded on PAM-18Na polymer against respiratory bacteria, including Klebsiella pneumoniae and Streptococcus pneumonia, and test the cytotoxicity of the prepared formula.

2. Materials and Methods

2.1. Materials

PAM-18Na polymer (250 gm Lot# MKCF 2071, Polymaleic Anhydride—Alt—Octadecene) with an average MW of 30,000–50,000 was obtained from Sigma-Aldrich, stored at room temperature. Ceftriaxone (PHARCO) is obtained from a pharmaceutical store. Additional chemicals and solvents with a high purity grade were purchased from commercial stores. The Regional Center for Mycology and Biotechnology at Al Azhar University generously provided the bacterial strains *Streptococcus pneumoniae* ATCC 49136 and *Klebsiella pneumoniae* ATCC 13883.

2.2. Nanoformulasynthesis

PAM-18Na polymer (25 gm) was added to 250 mL ultrapure water and was step wisely mixed with 250 mL of NaOH solution (1 M). This mixture was left for 24 hours with agitation using moderate magnetic stirring (200 rpm). One gram of a β -lactam drug (Ceftriaxone) was dissolved in 20 mL of ultrapure water, and the solution was slowly loaded onto the preprepared PAM-18Na polymer mixture for 24 hours with moderate magnetic stirring (200 rpm) until a translucent dispersion was obtained.

2.3. Characterizations

2.3.1. X-ray diffraction (XRD)

The XRD technique was applied to describe the crystallinity of the drug (Ceftriaxone), polymer (PAM-18Na), and formula by Cu Kα radiation (= 1.54 nm). The device is capable of scanning a range of two theta angles at a rate of 2 degrees per minute (step size = 0.050 degree and step time = 1.5 s) (10^o to 50^o) with an operating current of 30 mA and an operating voltage of 40 kV (power 1200 W). Using the corresponding International Centre for Diffraction Data cards, the crystalline phases could be identified. The crystallite size was determined from the XRD peaks using Scherrer's equation $D = \lambda/\beta \cos \theta$ (Eq. 1), where D stands for the mean crystallite size, λ is the radiation wavelength, β is the adjusted entire width at

half the maximum of the diffraction peak, θ is Bragg's diffraction angle.

2.3.2. Fourier transformation infrared spectroscopy (FTIR)

The functional groups were examined in drug (Ceftriaxone), polymer (PAM-18Na), and formula using FTIR from 4500 to 500 cm-1. To collect the FTIR spectra, a Bruker (Vertex 70 FTIR-FT Raman) spectrometer was used. The formula's spectra were gathered. Following three inspections, the spectra were averaged, and the scanning resolution was 1 cm^{-1}.

2.3.3. Morphology study

The surface morphology and particle size of the synthesized formula were determined by using a high-resolution transmission electron microscope (HRTEM, JEM 1400, software version DM 3, Japan) set to 300 kV.

2.3.4. Zetasizer and zeta potential measurements

The zeta potential, hydrodynamic size, polydispersity index value, and colloidal stability of the dispersed formula were determined by using photon correlation spectroscopy or dynamic light scattering (DLS) (Malvern, UK). With three measurements per run, all data analysis was carried out automatically.

2.3.5. Thermal gravimetric analysis (TGA)

Thermogravimetric differential thermal analysis (TGA-DTA) (Shimadzu Co., Tokyo, Japan) was used to measure thermal stability. The process involved heating a 50 mg sample of the formula to 1000 °C at a rate of 20 °C min^{-1} in a dynamic N2 environment.

2.4. Testing Antibacterial activity and Minimum Inhibitory concentration (MIC)

To evaluate the antibacterial impact of the drug (Ceftriaxone), polymer (PAM-18Na), formula, and gentamicin (a standard drug) versus *Streptococcus pneumonia* ATCC 49136 and *Klebsiella pneumonia* ATCC 13883, a standardized inoculum of the test organism is used to inoculate nutrient agar plates. The examined substances (1 mg/mL) are then inoculated on 6-mm-diameter filter paper discs and placed on the agar surface. The Petri dishes are incubated at 37 °C. Typically, an antimicrobial agent is diffused into the agar to inhibit bacterial growth, and the diameters of the zones of inhibition are measured [16].

The microdilution method was used to calculate the minimum inhibitory concentration (MIC) value of the antibiotic, polymer, and formula. In 96-well microtiter plates, 10 µL of log-phase culture was introduced after bacterial pathogens were cultured in sterile broth. 1% DMSO was used to dissolve various treatments, which were then serially diluted to achieve the desired concentrations (1 mg/mL–1.9 µg/mL).1%DEMSO was tested as negative control. A total of 200 µL of diluted fractions and sterile broth were added to pre-coated bacterial cultures. The plate was incubated at 37 °C for 18 hrs [17].

2.5. Ultrastructure examination of treated bacteria

After being treated with MIC concentrations of polymer and formula, *Streptococcus pneumonia* ATCC 49136 and Klebsiella pneumonia ATCC 13883 were fixed with 2.5% glutaraldehyde for two hours. The samples were next treated for two hours with 2% osmium tetroxide, and the blocks were dyed with 1% uranyl acetate before being dried with a graduated ethanol series. After that, resin was used to embed the samples. Using an ultra-microtome (Leica, Wetzkar, Germany), the materials were divided into slices. The sections (20µm thickness) were then examined under a transmission electron microscope (JOEL, Tokyo, Japan) [18].

2.6. Testing of cytotoxicity

In vitro 3-(4, 5-dimethylthiazol)-2-diphenyltetrazolium bromide (MTT) assays were performed to determine the toxicity of the formulation, polymer, and drug by measuring their effects on the viability of MRC-5 mammalian cells (normal human lung fibroblast cells). The tissue culture division at the holding company for biological products and vaccines (VACSERA), located in Giza, Egypt, was the source of the cell line used in this study. The cytotoxic effects were compared to that of the anticancer drug 5-fluorouracil (5-FU).

Cultivate the cells in RPMI medium on a 96-well plate for 48 hours, followed by a 6-hour starvation period. The tested formula was then serially diluted in the cell medium and administered to the cells, incubated in 5% CO2 incubator at 37°C for 48 hours. Each well received an addition of MTT, which was incubated for an additional 4 hours after the initial 48 hours at a fixed concentration of 0.5 mg/mL. The optical density absorbance was measured using a microplate reader (Bio-Rad Model 680, Hercules, CA, USA) at 590 nm after the solution was removed to determine the percentage of viable cells. The percentage of viability was calculated as [(ODt/ODc)] x 100%, where ODt is the mean optical density of wells treated with the tested sample and ODc is the mean optical density of untreated cells. The cytotoxicity was calculated using the percentage of cell viability. Measurements were taken three times throughout the test [19].

2.7. Statistical analysis

GraphPad Prism was used to analyze the data, which was given as means and standard deviations of means (SD) (version 5.0, San Francisco, USA). An unpaired, two-sided Student's t-test was utilized, and p $\leq$0.05 was taken into consideration to be statistically significant [20].

3. Results and Discussion

3.1. Qualitative analysis of XRD

The XRD patterns of Ceftriaxone, polymer PAM-18Na, and formula, are indicated in Fig.1. Ceftriaxone drug has sharp edges at 11.22 °, 12.66 °, 15.45 °, 18.45 °, 19.07 °, 20.12 °, 21.30 °, 22.87 °, 23.88 °, 25.30 °, 26.87 °, 27.86 °, 28.31 °, 29.68 °, 30.63 32.57°, 33.95°, 35.77°, 38.35°, 38.35°, 40.54°, 41.73°, 43.39°, 48.86° and 54.49°. The findings of the current study were consistent with those of a previous study [26, 27]. The polymer has sharp edges displaying a disordered arrangement of polymer chains, showing a wide diffuse hump peak at approximately 19.09° as shown by Salamanca et al., [28]. As depicted in Fig.1 the formula is in its crystal form, demonstrating the prepared formula's crystallinity. With a slight peak shift to the right and a change in the signal strength, the diffraction peaks hardly resemble those of Ceftriaxone. The observed similarity of the diffracted peaks between Ceftriaxone and the formula reflected the chemical structure integrity of the Ceftriaxone after loading. The shifting may be the result of modifications made to the structural design during the loading process, which may have changed the angle of interaction. The reported shift in the peak position of the diffracted peaks was also brought on by variations in the interatomic distance of the formula. Furthermore, the planar arrangement and interatomic distance discrepancies were brought on by ceftriaxone loading in polymer.

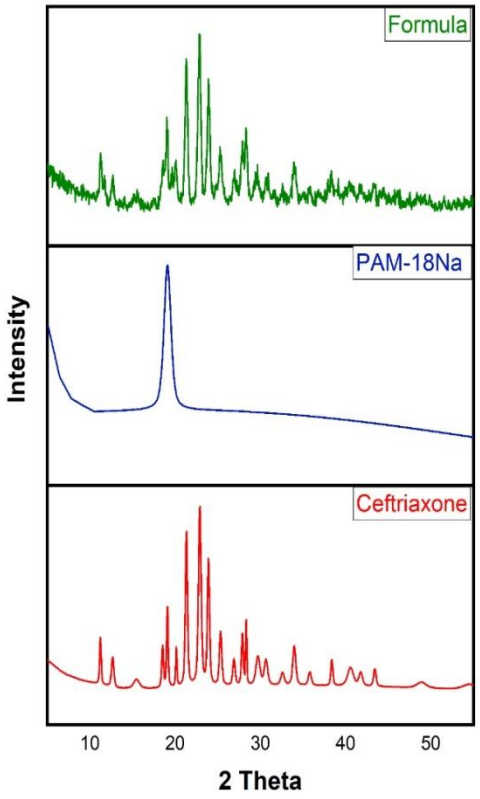

Fig. 1. XRD analysis of Formula, PAM-18Na polymer, and Ceftriaxone drug

3.2. FTIR spectra analysis

Figure 2 depicts the FTIR spectra of the Ceftriaxone, PAM-18Na polymer, and formula. The modest peak at 3431 cm-1, which is consistent with the overlapping of the stretching vibrations of the O-H and N-H groups, can be explained by the chemical

makeup of Ceftriaxone. The peak values are as follows: aliphatic C-H stretching (2933 cm-1), in-plane N-H bending vibration (1538 cm-1), primary alcoholic group C-O stretching vibration (1400 cm-1), and C3-OH hydroxyl group stretching vibration (1033 cm-1) [21, 22]. It is clear that the two spectra of the polymer (PAM-18Na) and formula shared a profile and displayed a variety of distinctive peaks with variations in their broadness and a non-significant shifting of the key peaks' positions. The creation of hydrogen bonds may be the cause of the change in the broadness between the polymer (PAM-18Na) and formula. The peaks in the polymer spectrum include a small band of OH groups at 2605 cm-1, -C-H stretching at 2925 cm-1, -C=C- symmetric aromatic ring stretching vibration (C=C ring) at 1458 cm-1, -O-H stretch at 1076 and 1225 cm-1, and -COOH carboxylic acid at 1719 cm-1. These peaks show that the IR spectra above are those of polymers. The resulting polymer's FTIR spectrum matched reports by other research groups. [23, 24]. The FTIR spectrum exhibits the well-known wide hydroxyl group peaks at 3605 cm-1 and 2925 cm-1, which are attributed to stretching CH3. The O-CH bond exhibits two absorption bands at 1458 cm-1 and 1225 cm-1. The C-O bond is primarily responsible for the complicated sequence of peaks in the spectral range between 1225 and 594 cm-1. Peaks at 1569 cm-1 and 1411 cm-1 were visible in the Ceftriaxone-polymer formula's FTIR spectra, suggesting the polymer's C=C aromatic, N-H/C-H stretching, and CH2 wagging coupled with OH groups. The large peak in the 3399–2924 cm-1 range denotes the establishment of a hydrogen bond between the ceftriaxone and polymer OH groups. In addition, the appearance of the distinctive peak at 1500 cm-1 supports the complex formation in accordance with Salamanca et al. [25] and suggests effective load capacity inside the polymeric matrix of the polymer.

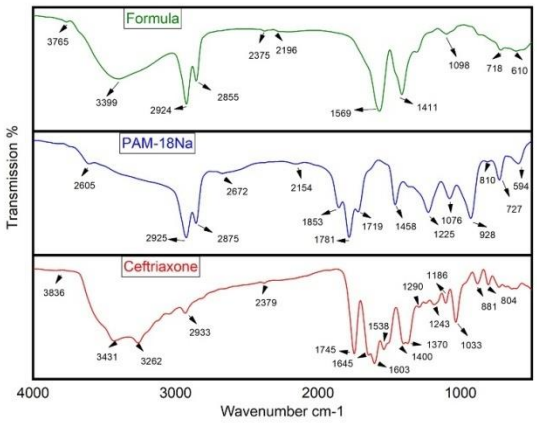

Fig. 2. FTIR spectra of Formula, PAM-18Na polymer, and Ceftriaxone drug.

3.3. Zetasizer and Zeta potential measurements

The hydrodynamic diameter of dispersed particles is commonly measured using the dynamic light scattering (DLS) method, which is a typical technique used to directly estimate the translational diffusion coefficient in the continuous phase. According to ISO 13321 [29], the Z-average size (or mean), commonly referred to as the cumulant mean, is the ideal figure to report when utilized in a quality-control situation. This hydrodynamic characteristic only applies to particles or molecules in dispersion or solution. The Z-average mean size could only be comparable to the size assessed by other approaches if the sample is unimodal, spherical or nearly spherical in shape, very narrow, and well prepared. The Z-average mean size can be sensitive to even tiny changes in the sample. The outcomes are depicted in Fig. 3A. The size distribution of drugs was found to be monomodal, w with a Z average of 294±0.89 nm. In contrast, Fig. 3C shows that polymers have a bimodal size distribution with a Z average of 129.9±0.64 nm. The Zeta potentials for the drug and polymer were found to be-24.4 mV and -47.5 mV, Fig 3B and Fig 3D, respectively. It is generally accepted that a zeta potential above +30 mV or below -30 mV provides adequate repulsion forces to prevent particle aggregation [30]. Concerning the formula (Fig. 3E), the reported hydrodynamic size, Polydispersity index PDI, and the intercept were 298 nm, 1.000, and 1.06, respectively. The PDI value indicated a narrow width, revealing homogenous size distribution. The zeta potential was -14.2 mV, showing low stability.

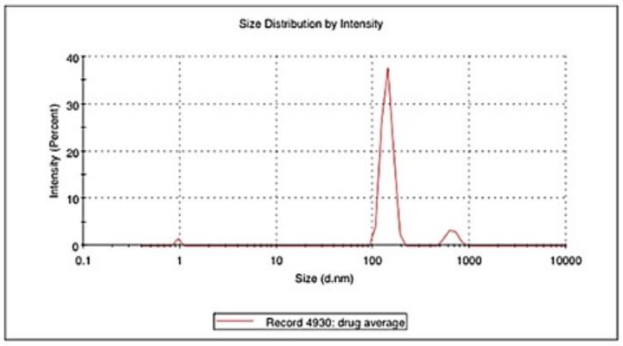

(A)

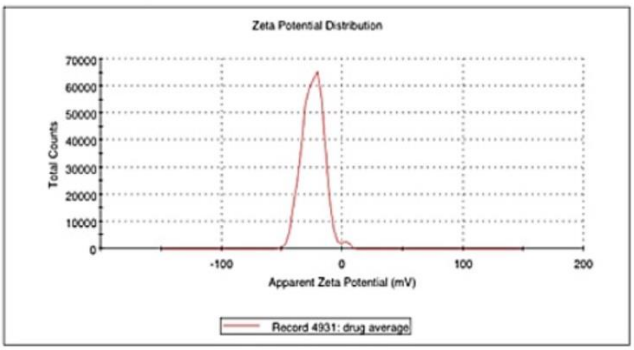

(B)

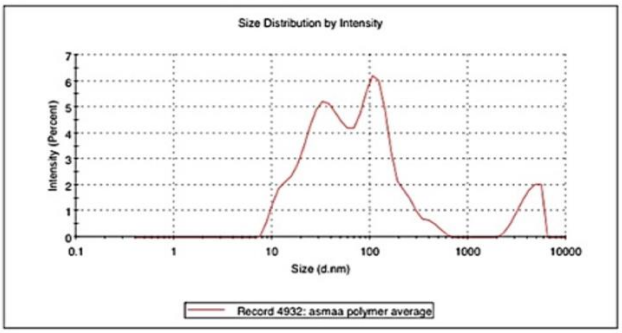

(C)

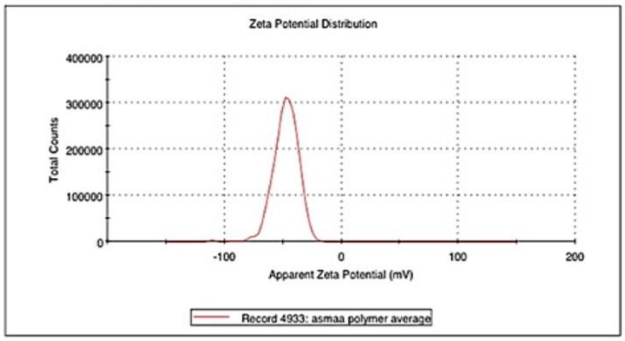

(D)

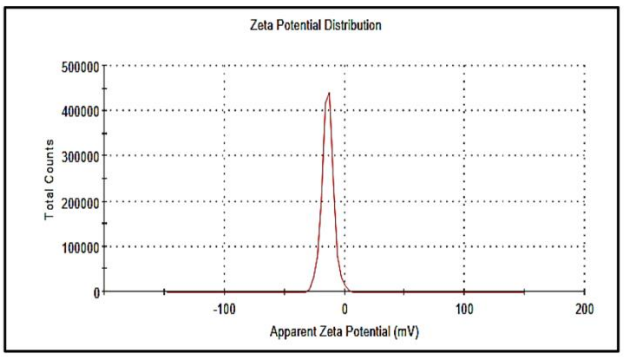

(E)

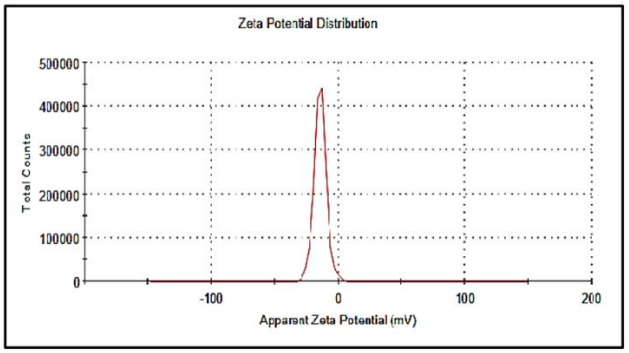

(F)

Fig.3.(A)- Zeta sizer drug, (B)- Zeta potential drug; (C)- Zeta sizer polymer, (D)- Zeta potential polymer, (E)- Zeta sizer formula, (F)- Zeta potential formula.

3.4. Thermodynamic Profiling of the formula (Polymer-Drug)

The results of the thermal characterization investigation of PAM-18Na polymer containing ceftriaxone are shown in Figure 4. From the DCS thermograms, it is possible to see a drop in the PAM-18Na formula's thermal transition temperature around 400 °C and a rise in the formula's thermal transition temperature around 600 °C, both of which become stronger with the addition of more formula. It is also possible to see the emergence of a new thermal signal that becomes more intense and energetic with the addition of more formula. These findings point to a strong interaction between ceftriaxone and the PAM-18Na polymer [31, 32, 33, 34].

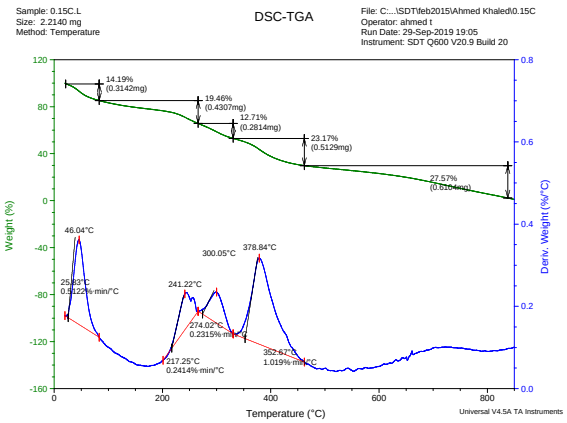

Fig.4.Thermal Gravimetric Analysis of the formula.

3.5. Transmission electron microscope examination for formula

Electron microscopy is vital for investigating the ionic, electrical, physical, biochemical, and other functional properties of advanced polymers and soft complexes, which has grown to be a potent and indispensable instrument. Loading ceftriaxone with a PAM-18Na polymer component can be imaged with a transmission electron microscope [35]. According to [36, 37], the HRTEM revealed an irregular shape with vacuoles (blue circle) of varying sizes within a range of 200 nm, as shown in Fig. 5 (A and B). It is possible that the contrasting dark and grey signal intensities seen in the photos result from differences in the attenuation of the input electron beam by Ceftriaxone and PAM-18Na polymer. Differences in electron density between ceftriaxone and PAM-18Na polymers are used to explain this attenuation, which proves that loading occurred. The HRTEM images show that Ceftriaxone has low lipophilicity, as seen by darker regions (green circle) inside the particles, which is the major limitation of all cephalosporin antibiotic drugs, while the grey regions may indicate soluble PAM-18Na polymers.

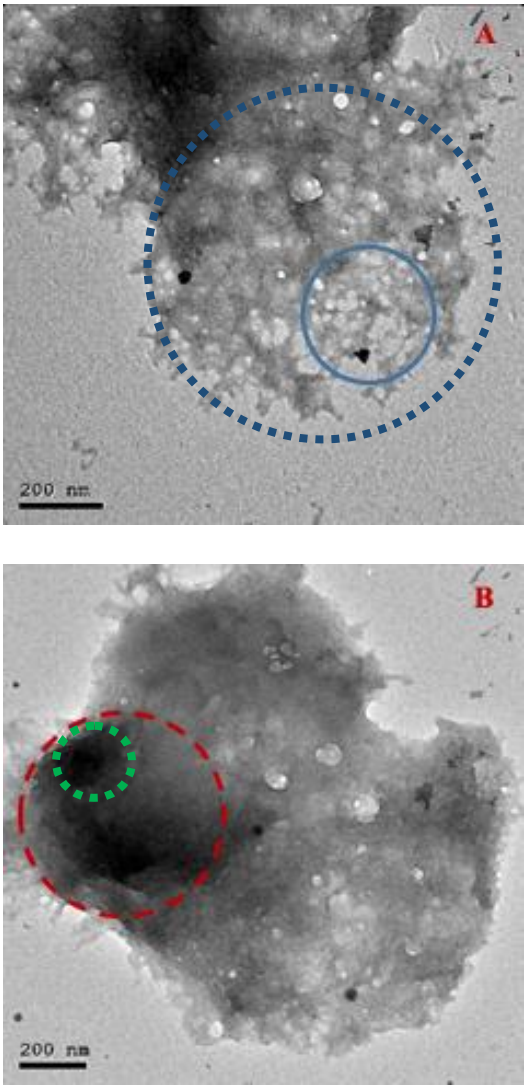

Fig.5.High-Resolution TEM images of two representative images of the prepared formula.

3.6. Biological studies

3.6.1. Antibacterial impact and MIC

An agar diffusion assay was applied to investigate the antibacterial action of a drug (Ceftriaxone), a polymer (PAM-18Na), a mixed formula, and gentamicin (a standard drug) versus *Streptococcus pneumoniae* and *Klebsiella pneumoniae*. The synthesized formula gave the highest inhibition zones compared to all cases at the same level of gentamicin. The inhibition zone of ceftriaxone versus *Streptococcus pneumonia* was 14.6 ±0.29 mm, while its inhibition zone versus *Klebsiella pneumonia* was 11.6 ±0.31 mm. Furthermore, the inhibition zone of the polymer had the inhibitory values versus *Streptococcus pneumonia* with 9.2 ±0.24 mm, while its inhibition zone versus *Klebsiella pneumonia* was 7.2 ±0.52 mm, as depicted in Table 1. As shown by other research groups [38-40], synthesized complexes can boost the efficacy of some antibiotics. Ceftriaxone had minimal inhibitory concertation 12.5, 15.6 µg/mL towards *Streptococcus pneumonia* and *Klebsiella pneumonia*, respectively. While PAM-18Na showed minimal inhibitory concertation of 250 µg/mL towards *Streptococcus pneumonia* or *Klebsiella pneumonia*. However, mixed formula had the best minimal inhibitory concertation with 1.905 and 3.905 µg/mL versus *Streptococcus pneumonia* and *Klebsiella pneumonia*, respectively, as shown in (Table 1). Chai et al., [41] reported the promising role of Polymyxin B-Polysaccharide Nano complex in improving the antibacterial activity against respiratory lung pathogens.

3.6.2. Examination of cellular variation using electron microscopy

Electron micrographs depict the cytological impact of MICs concentrations of polymer, or polymer-drug formula, on the Gram-positive bacteria *Streptococcus pneumonia*. The control cells in (Figure 6A) had intact plasma cell membranes and well-defined spherical outer cell boundaries, as well as dense inner cell walls. *Streptococcus pneumonia* treated with polymer, as observed in the electron micrograph,showed leakage and loss of cytoplasmic contents as well as the collapse of cells with smaller cell remnants (Figure 6B).

Table 1

Average inhibition zones in mm ± standard deviation, and minimum inhibitory concentrations (MICs) across all examined samples (Ceftriaxone, polymer, formula, and Gentamicin) against *Streptococcus pneumonia* and *Klebsiella pneumonia*.

	Streptococcuspneumonia		*Klebsiella pneumonia*	
	Inhibition Zone (mm)	MIC (µg/mL)	Inhibition Zone (mm)	MIC (µg/mL)
Ceftriaxone	14.6 ±0.29	12.5	11.6 ±0.31	15.6
Polymer	9.2 ±0.24	250	7.2 ±0.52	250
Formula	18.0 ±0.32	1.905	13.0 ±0.51	3.905
Gentamycin	16.78±0.46	6.25	12.65±0.71	12.5
1% DMSO	--	--	--	--

Amazingly, the mixed formula caused full cellular degeneration, with decreasing and vanishing cytoplasmic components eventually leading to cell death (Figure 6C).

The untreated (control) cells of Gram-negative bacteria K. pneumonia had a normal rod form; the cytoplasmic membrane was constantly in close contact with the cell wall, and the outer membrane of the cell wall exhibited a rigid appearance (Figure 6D). Polymer-induced cell damage; the cells had a larger periplasmic area between the outer and cytoplasmic membranes, as shown in (Figure 6E).

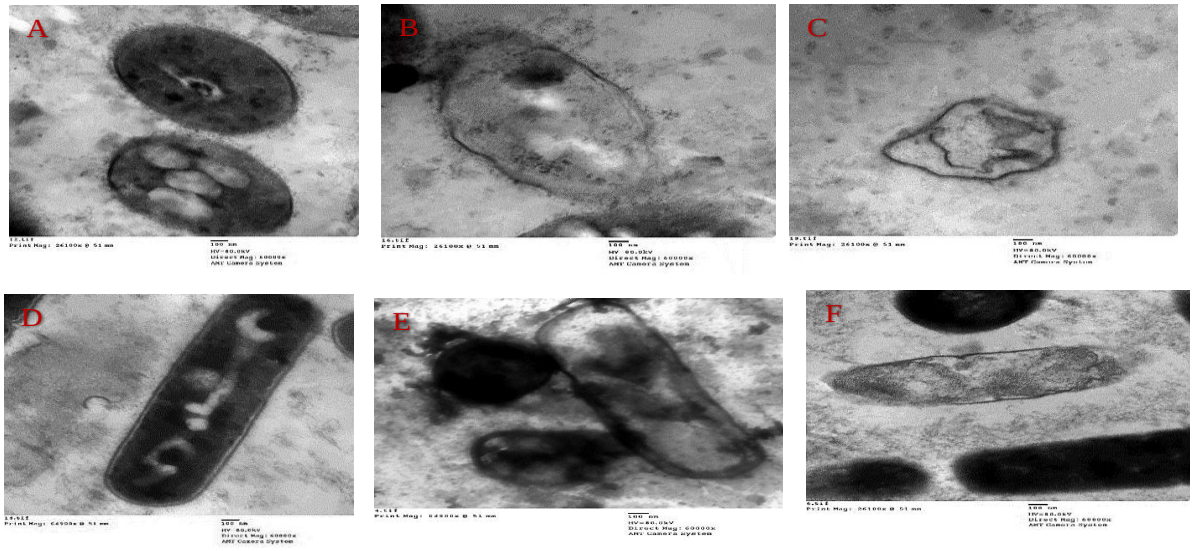

Fig. 6. Transmission electron microscopy images of *Streptococcus pneumonia*(A) Control; (B) *Streptococcuspneumonia*treated by polymer; (C) *Streptococcuspneumonia*treated by the mixed formula; *Klebsiella pneumoniae* (D) Control; (E) *Klebsiella pneumoniae* affected by polymer (F) *Klebsiella pneumoniae* affected by the mixed formula.

leaks, as dramatic observations had been seen with the effect of the synthesized formula (Figure 6F)
The vital significance that ultrastructural morphology, histochemistry, and microanalysis play in the advancement of nanomedicine was recently underlined by Malatesta et al. [42]. These techniques were used to study how nanostructures influence living things. Furthermore, Carton et al. [43] reported the antimicrobial role of nanoparticles through investigation using electron microscopy.

3.6.3. Cytotoxicity examination

The cytotoxicity of the investigated materials was studied in relation to normal cell lines to ensure their safety for medicinal applications. In this study, the cytotoxicity of ceftriaxone, PAM-18Na, and formula against the MRC-5 cell line was analyzed using the MTT assay. When using Ceftriaxone as an approved comparative drug, the 50% cytotoxic concentration (CC50) value was 482.61± 12.37 µg/mL. Furthermore, the CC50 concentrations of PAM-18Na and formula towards the MRC-5 normal cell line were 731.03 ± 23.79 µg/mL and 960.12± 29.04 µg/mL, respectively, as illustrated in Figure 7. In accordance with Bonferoni et al., [44] it was reported that chitosan and its analogues could precisely through passive and active targeting while causing the least amount of cytotoxicity due to their unique surface features. Furthermore, Wang et al. [45] investigated steady loading, side effect shielding, and tumor-targeted delivery with low cytotoxicity through the use of many nanocarrier technologies.

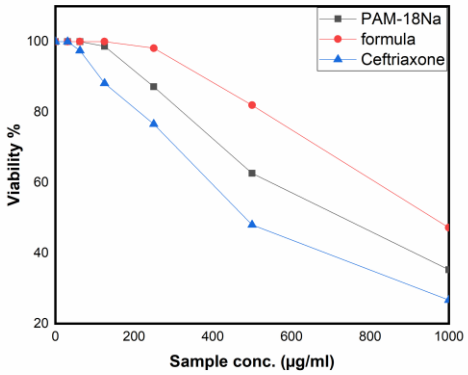

Fig.7.Cytotoxicity assay versus MRC-5 where, (Ceftriaxone) CC50 = 482.61± 12.37 µg/mL; (B2: PAM-18Na) CC50 = 731.03 ± 23.79 µg/mL and formula (drug-polymer) CC50 = 960.12± 29.04 µg/mL.

4. Conclusion

In the current investigation, the ceftriaxone antibiotic was synthesized as a hydrophilic drug and loaded onto the PAM-18Na polymer using a nanostructured formula. *Streptococcus pneumonia* and *Klebsiella pneumonia* were used in the investigation of the formula's impact on bacterial structure and potency using testing on normal cell lines. The developed solution has the potential to replace the current standard treatment for common bacterial lung infections.

5. Conflicts of interest

There are no conflicts to declare.

6. Formatting of funding sources

The current study received no institutional financial fund, and it was maintained through individual funding.

7. References

[1] Yeh YC, Huang TH, Yang SC, Chen CC, Fang JY. Nano-Based Drug Delivery or Targeting to Eradicate Bacteria for Infection Mitigation: A Review of Recent Advances. Front Chem. 2020; 8:286. doi: 10.3389/fchem.2020.00286.

[2] Fadaka AO, Sibuyi NRS, Madiehe AM, Meyer M. Nanotechnology-Based Delivery Systems for Antimicrobial Peptides. Pharmaceutics. 2021;13(11):1795. doi: 10.3390/pharmaceutics13111795.

[3] Smith R.A., M'ikanatha N.M., Read A.F. Antibiotic resistance: A primer and call to action. Health Commun. 2015; 30:309–314. doi: 10.1080/10410236.2014.943634.

[4] Jasovský D., Littmann J., Zorzet A., Cars O. Antimicrobial resistance—A threat to the world's sustainable development. Upsala J. Med. Sci. 2016; 121:159–164. doi: 10.1080/03009734.2016.1195900.

[5] Prestinaci F., Pezzotti P., Pantosti A. Antimicrobial resistance: A global multifaceted phenomenon. Pathog. Glob. Health. 2015; 109:309–318. doi: 10.1179/2047773215Y.0000000030.

[6] Natan M., Banin E. From Nano to Micro: Using nanotechnology to combat microorganisms and their multidrug resistance. FemsMicrobiol. Rev. 2017; 41:302–322. doi: 10.1093/femsre/fux003

[7] Deng Y., Huang R., Huang S., Xiong M. Nanoparticles Enable Efficient Delivery of Antimicrobial Peptides for the Treatment of Deep Infections. BIO Integr. 2021 doi: 10.15212/bioi-2021-0003.

[8] Baptista P. V., McCusker M. P., Carvalho A., Ferreira D. A., Mohan N. M., Martins M., et al. (2018). Nano-strategies to fight multidrug resistant bacteria- "A battle of the Titans". Front. Microbiol. 9:1441 10.3389/fmicb.2018.01441

[9] Taylor E., Webster T.J. (2011). Reducing infections through nanotechnology and nanoparticles. Int. J. Nanomed. 6, 1463–1473. 10.2147/IJN.S22021

[10] Zazo H., Colino C. I., Lanao J. M. (2016). Current applications of nanoparticles in infectious diseases. J. Control. Release 224, 86–102. 10.1016/j.jconrel.2016.01.008

[11] Walvekar P., Gannimani R., Govender T. (2019). Combination drug therapy via nanocarriers against infectious diseases. Eur. J. Pharm. Sci. 127, 121–141. 10.1016/j.ejps.2018.10.017

[12] Salamanca C., Barraza R.G., Acevedo B., Olea A.F. Hydrophobically modified polyelectrolytes as potential drugs reservoirs of N-alkyl-nitroimidazoles. J. Chil. Chem. Soc. 2007;52 doi: 10.4067/S0717-97072007000100014.

[13] Salamanca CH, Yarce CJ, Roman Y, Davalos AF, Rivera GR. Application of Nanoparticle Technology to Reduce the Anti-Microbial Resistance through β-Lactam Antibiotic-Polymer Inclusion Nano-Complex. Pharmaceuticals (Basel). 2018 Feb 10;11(1):19. doi: 10.3390/ph11010019.

[14] Kim L, McGee L, Tomczyk S, Beall B. Biological and Epidemiological Features of Antibiotic-Resistant Streptococcus pneumoniae in Pre- and Post-Conjugate Vaccine Eras: a United States Perspective. Clin Microbiol Rev. 2016;29(3):525-552. doi:10.1128/CMR.00058-15

[15] Heng ST, Chen SL, Wong JGX, Lye DC, Ng TM. No association between resistance mutations, empiric antibiotic, and mortality in ceftriaxone-resistant Escherichia coli and Klebsiella pneumoniae bacteremia. Sci Rep. 2018;8(1): 12785. doi:10.1038/s41598-018-31081-6

[16] Balouiri M, Sadiki M, Ibnsouda SK. Methods for in vitro evaluating antimicrobial activity: A review. J Pharm Anal. 2016 Apr;6(2):71-79. doi: 10.1016/j.jpha.2015.11.005.

[17] Siddharth S, Vittal RR. Evaluation of Antimicrobial, Enzyme Inhibitory, Antioxidant and Cytotoxic Activities of Partially Purified Volatile Metabolites of Marine Streptomyces sp.S2A.

Microorganisms. 2018;6(3):72. doi: 10.3390/microorganisms6030072.
[18] Teodori L., Tagliaferri F., Stipa F., Valente M.G., Coletti D., Manganelli A., et al. Selection, establishment and characterization of cell lines derived from a chemically-induced rat mammary heterogeneous tumor, by flow cytometry, transmission electron microscopy, and immunohistochemistry. In Vitro Cell Dev Biol Anim. 2000; 36:153–162. doi: 10.1290/1071-2690(2000)036<0153: SEACOC>2.0.CO;2.
[19] Berridge MV, Herst PM, Tan AS. Tetrazolium dyes as tools in cell biology: new insights into their cellular reduction. BiotechnolAnnu Rev. 2005; 11:127–152. doi: 10.1016/S1387-2656(05)11004-7
[20] Sayed R, Safwat NA, Amin BH, Yosri M. Study of the dual biological impacts of aqueous extracts of normal and gamma-irradiated Galleria mellonella larvae. J Taibah Univ Med Sci. 2022;17(5):765-773. doi: 10.1016/j.jtumed.2021.12.016.
[21] Ebrahimi, S., Farhadian, N., Karimi, M. et al. Enhanced bactericidal effect of ceftriaxone drug encapsulated in nanostructured lipid carrier against gram-negative Escherichia coli bacteria: drug formulation, optimization, and cell culture study. Antimicrob Resist Infect Control 9, 28 (2020). https://doi.org/10.1186/s13756-020-0690-4
[22] Alshammari F, Alshammari B, Moin A, Alamri A, Al Hagbani T, Alobaida A, Baker A, Khan S, Rizvi SMD. Ceftriaxone Mediated Synthesized Gold Nanoparticles: A Nano-Therapeutic Tool to Target Bacterial Resistance. Pharmaceutics. 2021 Nov 8;13(11):1896. doi: 10.3390/pharmaceutics13111896
[23] Olea A.F., Barraza R., Fuentes I., Acevedo B. Solubilization of Phenols by Intramolecular Micelles Formed by Copolymers of Maleic Acid and Olefins. Macromolecules. 2002; 35:1049–1053. doi: 10.1021/ma0108362.
[24] Salamanca C., Barraza R.G., Acevedo B., Olea A.F. Hydrophobically modified polyelectrolytes as potential drugs reservoirs of N-alkyl-nitroimidazoles. J. Chil. Chem. Soc. 2007;52 doi: 10.4067/S0717-97072007000100014.
[25] Salamanca CH, Yarce CJ, Roman Y, Davalos AF, Rivera GR. Application of Nanoparticle Technology to Reduce the Anti-Microbial Resistance through β-Lactam Antibiotic-Polymer Inclusion Nano-Complex. Pharmaceuticals (Basel). 2018 Feb 10;11(1):19. doi: 10.3390/ph11010019.
[26] Jeon O-C, et al. Oral delivery of ionic complex of ceftriaxone with bile acid derivative in non-human primates. Pharm Res. 2013;30(4):959–67.
[27] Carrillo-Navas H, et al. Shear rheology of water/glycerol monostearate crystals in canola oil dispersions interfaces. Colloids Surf APhysicochemEng Asp. 2013; 436:215–24.
[28] Salamanca CH, Yarce CJ, Zapata CA, Giraldo JA. Relationship between the Polymeric Ionization Degree and Powder and Surface Properties in Materials Derived from Poly (maleic anhydride-alt-octadecene). Molecules. 2018;23(2). doi:10.3390/molecules23020320
[29] Salamanca C.H., Castillo D.F., Villada J.D., Rivera G.R. Physicochemical characterization of in situ drug-polymer nanocomplex formed between zwitterionic drug and ionomeric material in aqueous solution. Mater. Sci. Eng. C. 2017;72 doi: 10.1016/j.msec.2016.11.097.
[30] Clogston JD, Patri AK. Zeta potential measurement. Methods Mol Biol. 2011; 697:63-70. doi: 10.1007/978-1-60327-198-1_6.
[31] Colzi I., Troyan A.N., Perito B., Casalone E., Romoli R., Pieraccini G., Škalko-Basnet N., Adessi A., Rossi F., Gonnelli C., et al. Antibiotic delivery by liposomes from prokaryotic microorganisms: Similia cum similis works better. Eur. J. Pharm. Biopharm. 2015; 94:411–418. doi: 10.1016/j.ejpb.2015.06.013.
[32] Muppidi K., Pumerantz A., Wang J., Betageri G. Development and stability studies of novel liposomal vancomycin formulations. Arch. ISRN Pharm. 2012; 2012:636743. doi: 10.5402/2012/636743.
[33] Turos E., Reddy G., Greenhalgh K. Penicillin-Bound Polyacrylate Nanoparticles: Restoring the Activity of β-Lactam Antibiotics Against MRSA. Bioorg. Med. Chem. Lett. 2007; 17:3468–3472. doi: 10.1016/j.bmcl.2007.03.077.
[34] Turos E., Shim J.-Y., Wang Y., Greenhalgh K., Reddy G.S.K., Dickey S., Lim D.V. Antibiotic-conjugated polyacrylate nanoparticles: New opportunities for development of anti-MRSA agents. Bioorg. Med. Chem. Lett. 2007; 17:53–56. doi: 10.1016/j.bmcl.2006.09.098.
[35] Chen J., Das S., Shao M., Li G., Lian H., Qin J., James F., Browning J., Keum K., David U., et al. Phase segregation mechanisms of small molecule-polymer blends unraveled by varying polymer chain architecture. SmartMat. 2021:1–11. doi: 10.1002/smm2.1036.
[36] Chen J., Yu X., Hong K., Messman J.M., Pickel D.L., Xiao K., Dadmun M.D., Mays J.W., Rondinone A.J., Sumpter B.G., et al. Ternary Behavior and Systematic Nanoscale Manipulation of Domain Structures in P3HT/PCBM/P3HT-b-PEO Films. J. Mater. Chem. 2012; 22:13013–13022. doi: 10.1039/c2jm31124k.
[37] Chen J. Advanced Electron Microscopy of Nanophased Synthetic Polymers and Soft Complexes for Energy and Medicine Applications.

Nanomaterials (Basel). 2021 Sep 15;11(9):2405. doi: 10.3390/nano11092405.
[38] Kamaruzzaman N., Pina M., Chivu A., Good L. Polyhexamethylene biguanide and nadifloxacin self-assembled nanoparticles: Antimicrobial effects against intracellular methicillin-resistant Staphylococcus aureus. Polymers. 2018; 10:521. doi: 10.3390/polym10050521.
[39] Kamaruzzaman N.F., Tan L.P., Hamdan R.H., Choong S.S., Wong W.K., Gibson A.J., Chivu A., Pina M.F. Antimicrobial Polymers: The Potential Replacement of Existing Antibiotics? Int. J. Mol. Sci. 2019; 20:2747. doi: 10.3390/ijms20112747.
[40] Edis Z, Haj Bloukh S, Ibrahim MR, Abu Sara H. "Smart" Antimicrobial Nano complexes with Potential to Decrease Surgical Site Infections (SSI). Pharmaceutics. 2020 Apr 15;12(4):361. doi: 10.3390/pharmaceutics12040361.
[41] Chai M, Gao Y, Liu J, Deng Y, Hu D, Jin Q, Ji J. Polymyxin B-Polysaccharide Polyion Nanocomplex with Improved Biocompatibility and Unaffected Antibacterial Activity for Acute Lung Infection Management. Adv Healthc Mater. 2020 Feb;9(3): e1901542. doi: 10.1002/adhm.201901542.
[42] Malatesta M. Transmission Electron Microscopy as a Powerful Tool to Investigate the Interaction of Nanoparticles with Subcellular Structures. Int J Mol Sci. 2021 Nov 26;22(23):12789. doi: 10.3390/ijms222312789.
[43] Carton F., Repellin M., Lollo G., Malatesta M. Alcian blue staining to track the intracellular fate of hyaluronic-acid-based nanoparticles at transmission electron microscopy. Eur. J. Histochem. 2019; 63:3086. doi: 10.4081/ejh.2019.3086.
[44] Bonferoni MC, Gavini E, Rassu G, Maestri M, Giunchedi P. Chitosan Nanoparticles for Therapy and Theranostics of Hepatocellular Carcinoma (HCC) and Liver-Targeting. Nanomaterials (Basel). 2020 Apr 30;10(5):870. doi: 10.3390/nano10050870.
[45] Wang A, Zheng Y, Zhu W, Yang L, Yang Y, Peng J. Melittin-Based Nano-Delivery Systems for Cancer Therapy. Biomolecules. 2022 Jan 12;12(1):118. doi: 10.3390/biom12010118.